

On the formation mechanisms of the diffuse atmospheric pressure dielectric barrier discharge
in CVD processes of thin silica-like films

This article has been downloaded from IOPscience. Please scroll down to see the full text article.

2009 Plasma Sources Sci. Technol. 18 045021

(<http://iopscience.iop.org/0963-0252/18/4/045021>)

View [the table of contents for this issue](#), or go to the [journal homepage](#) for more

Download details:

IP Address: 131.180.130.109

The article was downloaded on 08/08/2011 at 09:54

Please note that [terms and conditions apply](#).

On the formation mechanisms of the diffuse atmospheric pressure dielectric barrier discharge in CVD processes of thin silica-like films

S A Starostin^{1,2}, P Antony Premkumar^{1,2}, M Creatore²,
E M van Veldhuizen², H de Vries³, R M J Paffen³ and
M C M van de Sanden²

¹ Materials Innovation Institute (M2i), Mekelweg 2, 2600 GA Delft, The Netherlands

² Department of Applied Physics, Eindhoven University of Technology, 5600 MB Eindhoven, The Netherlands

³ FUJIFILM Manufacturing Europe B.V, PO Box 90156, Tilburg, The Netherlands

Received 23 March 2009, in final form 16 July 2009

Published 11 September 2009

Online at stacks.iop.org/PSST/18/045021

Abstract

Pathways of formation and temporal evolution of the diffuse dielectric barrier discharge at atmospheric pressure were experimentally studied in this work by means of optical (fast imaging camera) and electrical diagnostics. The chosen model system is relevant for applications of plasma-enhanced chemical vapor deposition of thin silica-like film on the polymeric substrate, from cost-efficient gas mixtures of Ar/N₂/O₂/hexamethyldisiloxane. It was found that the discharge can gradually experience the phases of homogeneous low current Townsend-like mode, local Townsend to glow transition and expanding high current density ($\sim 0.7 \text{ A cm}^{-2}$) glow-like mode. While the glow-like current spot occupies momentarily only a small part of the electrode area, its expanding behavior provides uniform treatment of the whole substrate surface. Alternatively, it was observed that a visually uniform discharge can be formed by the numerous microdischarges overlapping over the large electrode area.

(Some figures in this article are in colour only in the electronic version)

1. Introduction

The diffuse atmospheric pressure dielectric barrier discharge (DBD) [1] is nowadays recognized as a promising tool for plasma-enhanced chemical vapor deposition (PECVD) of thin films on several substrates [2–10]. The main benefit of PECVD at atmospheric pressure is the potential of cost-efficient in-line production without expensive and bulky vacuum equipment, required for running the conventional low-pressure process. However, the ignition and sustaining of high power uniform non-thermal atmospheric discharges over a large surface area impose serious scientific and technological challenges.

The DBD is a common source of non-thermal plasma at atmospheric pressure [11]. In the standard DBD system the discharge is ignited by applying a variable voltage between two metal electrodes, one or both of them being

covered by a solid dielectric layer. The purpose of the dielectric layer is to limit transferred charge and conduction current value, avoiding transition to an arc discharge. When compared with other sources of atmospheric non-thermal plasma [12, 13], e.g. corona discharge or atmospheric pressure plasma jets (APPJ), the DBD is characterized by low gas consumption, considerably high specific power deposition and strong potential for up scaling. Unfortunately, the most common type of high-pressure DBD is non-uniform and filamentary. The existence of the uniform diffuse modes of DBD (suitable for high-pressure PECVD) is usually strongly limited by the use of a specific gas mixture composition, dissipated power, operation frequency, etc. Two different kinds of diffuse atmospheric DBDs are presently in focus and of significant research interest: the low current atmospheric pressure Townsend-like discharge (APTD) [2] and the high

current atmospheric pressure glow-like discharge (APGD) [1, 3, 4]. The typical current densities for APTD are around 0.5 mA cm^{-2} , while for the APGD current densities are $\sim 100 \text{ mA cm}^{-2}$. APGD provides higher dissipated specific power densities compared with APTD, thus, being more compatible with plasma-enhanced high rate deposition processes.

The mechanisms leading to the formation of the diffusive glow-like DBD modes are still the subject of scientific research and discussion. Mangolini *et al* [14] studied the glow-like discharge development in He by means of fast imaging and space-resolved current measurements with sectioned electrodes. It was found that first a relatively large diffuse glow-like current spot a few centimeters in diameter is formed, followed by a ring-like expansion. A similar behavior for APGD in He was observed by Luo *et al* [15], who also demonstrated that initially a subnormal glow-like current spot appears by the transition from the low current Townsend-like discharge. Two-dimensional fluid modeling performed by Golubovskii *et al* [16] for a DBD in nitrogen indicates that the Townsend–glow transition can occur via a narrow cathode-directed streamer, which would form an initial glow-like cathode spot. Depending on the external electrical circuit this spot may expand over larger areas. Rahel *et al* [17] investigated the visually uniform DBD discharge in air by registering time-resolved emission with a photomultiplier and recording discharge current. They concluded that the discharge pattern developed similarly to that described by Golubovskii's model [16]. Yet no fast imaging was reported in [17] to directly verify the glow-like discharge character. It was shown in [18] that at a high density of non-stationary streamers the discharge can also have a diffusive appearance. In our preliminary investigation on the atmospheric pressure DBD temporal evolution in an Ar/N₂/O₂/hexamethyldisiloxane gas mixture [19] we confirmed a formation of the expanding glow-like discharge in the depositing plasma by means of fast imaging. However, no analysis of the electrical characteristics was presented in this brief communication.

It should be emphasized that the majority of investigations on the APGD assisted CVD process for inorganic thin films, which were presented up to now in the literature, are using helium as a carrying gas for reactive admixtures. The reported experimental research on the formation and temporal evolution of the atmospheric glow-like discharges at the nanosecond time scale are also mainly focused on the He-based gas mixtures. Yet, those results cannot be readily generalized for any arbitrary gas mixture. The specific properties of helium and discharges in helium are large thermal conductivity, low normal current density (for instance, for steel electrodes $J(\text{He}) = 2.2 \mu\text{A} (\text{cm}^{-2} \text{ Torr}^{-2})$ and $J(\text{N}_2) = 400 \mu\text{A} \text{ cm}^{-2} \text{ Torr}^{-2}$ [20]) and easier discharge ignition due to the efficient production of the secondary electrons at the cathode surface by metastables. The combination of these properties leads to a suppression of the instabilities typical for high pressure discharges, while arbitrary and especially electronegative gas mixtures can be very prone to transition to the non-uniform filamentary mode, which might be undesirable for film deposition. However, helium-based atmospheric pressure deposition processes are hardly

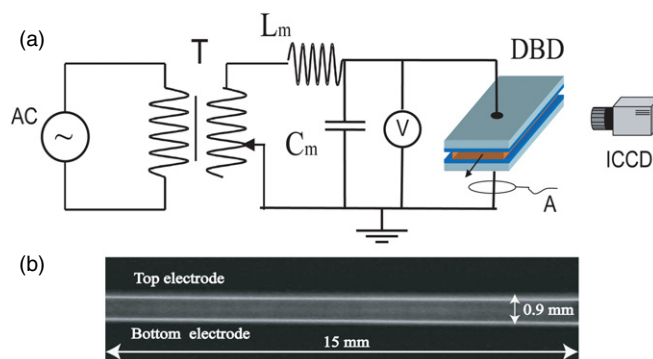


Figure 1. (a) Schematic of the experimental setup. DBD and ICCD are the DBD cell and fast imaging camera. Arrow shows the direction of gas flow. T, L_m and C_m indicate step transformer, inductive and capacitive matching elements, respectively. V and A denote positions of the voltage and current probes. (b) Typical appearance of the diffuse atmospheric pressure DBD recorded at 10 ms exposure time.

acceptable for large-scale industrial applications, because of the high gas costs and required recirculation system with efficient exhaust gas purification from volatile PECVD products.

All these considerations therefore support the study of the diffuse glow-like discharge operation and formation mechanisms under experimental conditions very close to practical applications and in cost-efficient gas mixtures. This research is complemented by the recent detailed analysis of the surface morphology and composition performed for thin silica-like films web-roll deposited in a similar discharge system [3, 4].

2. Experimental

A schematic of the experimental setup is presented in figure 1(a). The DBD was ignited between two plane-parallel stainless steel electrodes, both covered with a dielectric polymer foil. The discharge volume was provided with a system of uniform gas flow injection and was open to ambient air at the gas exhaust side. For the ICCD imaging experiments presented here the discharge area was $40 \times 12 \text{ mm}^2$. The discharge area was reduced compared with our previously reported thin film deposition experiment [3] in order to provide sufficient optical resolution of the discharge transverse structure. The gaseous gap size was varied between 0.6 and 1.2 mm. A polymer foil of polyethylene-2,6 naphthalate (PEN) ($100 \mu\text{m}$ thick) treated in the discharge served the purpose of a dielectric barrier, having a direct contact with the metal electrodes.

The DBD was powered by a high frequency sine wave generator (Seren Industrial Power Systems L2001). The electrical circuit included a step transformer (Seren MT1U) and the matching elements L_m and C_m (see figure 1(a)). The electrical characteristics of the discharge were monitored by an oscilloscope (Tektronix TDS 3034B) equipped with a voltage (Tektronix P6015A) and current (Tektronix P6016) probe.

The discharge operational frequency was tuned in the interval of 120–140 kHz to obtain better matching. Typical

voltage amplitude between the electrodes was 2-3 kV and the area-averaged current density corresponding to current peak maximum was $\sim 100 \text{ mA cm}^{-2}$. The characteristic period averaged value of the dissipated power was in the range $\sim 10\text{--}15 \text{ W cm}^{-2}$.

The gas mixture used in this investigation contained argon and nitrogen as carrier gases, oxygen as an oxidizer and hexamethyldisiloxane (HMDSO) as a deposition precursor for silica-like films according to the following dilution ratio: $\text{Ar/N}_2/\text{O}_2 + \text{HMDSO } 80/20/2 + 50 \text{ ppm}$ [3]. The gas flow rate was 0.5 slm directed along the 40 mm side of the discharge volume. The HMDSO precursor was injected using a controlled evaporation mixer coupled to a liquid mass flowmeter (Bronkhorst Liqui-Flow). As mentioned above, the buffer gas mixture consists of argon and nitrogen. The reason for using Ar is that this non-expensive and standard for plasma technology noble gas ($\sim 1\%$ in atmospheric air) provides operation of the discharge system at relatively low ac voltage amplitudes. From our experience we know that the addition of nitrogen improves the quality of the deposited silica-like films (in terms of residual carbon content and film density). This may occur via the contribution of the metastable nitrogen produced in plasma to the fragmentation of the HMDSO precursor as well as to the dissociation of molecular oxygen into atomic oxygen radicals. Those mechanisms are still under investigation.

The typical visual appearance of the diffuse DBD in a 0.9 mm gaseous gap during the deposition process of thin silica-like films [3, 4] recorded by a conventional digital camera at 10 ms exposure time is shown in figure 1(b). The discharge forms two bright layers near the surface of dielectric barriers, while the bulk region is less bright and the filamentation is not visible.

Fast imaging measurements of the discharge temporal development were performed by an ICCD camera (Andor DH734-18F) with the shortest gate time being 5 ns. Each of the presented ICCD image frames is independently normalized to its maximum intensity. In order to show the variation of the discharge brightness in time we also plotted the integral of the emitted light (recorded over ICCD pixels) as a function of time. In this way the ICCD camera acts as a conventional photomultiplier. Furthermore, each presented image frame in the discharge development sequence is recorded for a particular discharge event. The apparent visual relation between the images indicates the reproducibility of the discharge development pattern.

3. Results and discussion

Since the terminology in the field of diffuse atmospheric pressure DBDs is not entirely established, especially considering glow-like and Townsend-like modes, in this paper we will follow the definitions generally adopted in low-pressure gas discharge physics [20] and also used for uniform discharges at atmospheric pressure [21].

The classical Townsend or dark discharge is a low current self-sustained discharge characterized by a relatively small space charge which does not affect the external electric field.

The electric field in this case is constant across the discharge gap. The operating voltage of the Townsend discharge is close to the breakdown voltage, while the process of step ionization from accumulated atomic or molecular excited states will eventually reduce the voltage as current increases. According to Townsend's theory the electron density exponentially grows from cathode to anode producing a higher density of the excited states and noticeable light emission in the anode region [20]. The sources of the secondary electrons at the cathode are ion-electron secondary emission and photoemission, while photo-ionization, Penning ionization and electron emission induced by the excited particles should also be considered. The stationary Townsend discharge will occupy the whole area of the plane-parallel electrodes because the electron multiplication in the case of a uniform field does not depend on the current density.

As the discharge current increases, the positive space charge, initially accumulated in the anode region due to the difference in mobilities of the electrons and positive ions, will start to affect the electric field profile. This will lead to the enhancement of the field and ionization rate in the cathode direction, resulting in the formation of the fast propagating ionization wave directed from the anode to the cathode. Finally a glow discharge is established, characterized by the considerable positive space charge in the region next to the cathode, which in turn is producing a strong electric field variation known as cathode voltage fall. The recognizable property of the subnormal and normal glow discharges is that they will *not* occupy the whole electrode area, but will form the localized cathode spot. This is related to the fact that in the glow discharge the electron multiplication depends on the current density, because the electric field distribution is affected by the space charge. Moreover, at certain values of the reduced electric field $(E/p)_s$ (Stoletov point) [20], electron multiplication reaches its maximum. The last situation is realized in the cathode sheath of a normal glow discharge.

A glow discharge is characterized by the high electric field in the cathode layer and a lower field in the bulk region. The region of the high field will, in turn, result in relatively high electron energies, excited state densities and light emission. The light emission pattern from the cathode layer of the low-pressure glow discharge is rather complex [20] due to the spatial variations in electron number density and electron energy distribution function. The fine details of this layered pattern become indistinguishable at elevated gas pressures, but usually the bright sheath observed near the cathode is attributed to the negative glow (NG) which is positioned at the end of the cathode voltage fall. The NG is followed by the region with low electric field and luminosity known as a Faraday dark space. Then, the field rises again and the plasma luminosity increases in the bulk region. Following these distributions we conclude that the discharge luminosity pattern and the current density can indicate the operating mode of the diffuse atmospheric pressure DBD.

While APTD and APGD in the presence of dielectric barrier were named because of the close similarity to the traditional direct current Townsend and glow discharges between metal electrodes, the term 'filamentary' discharge

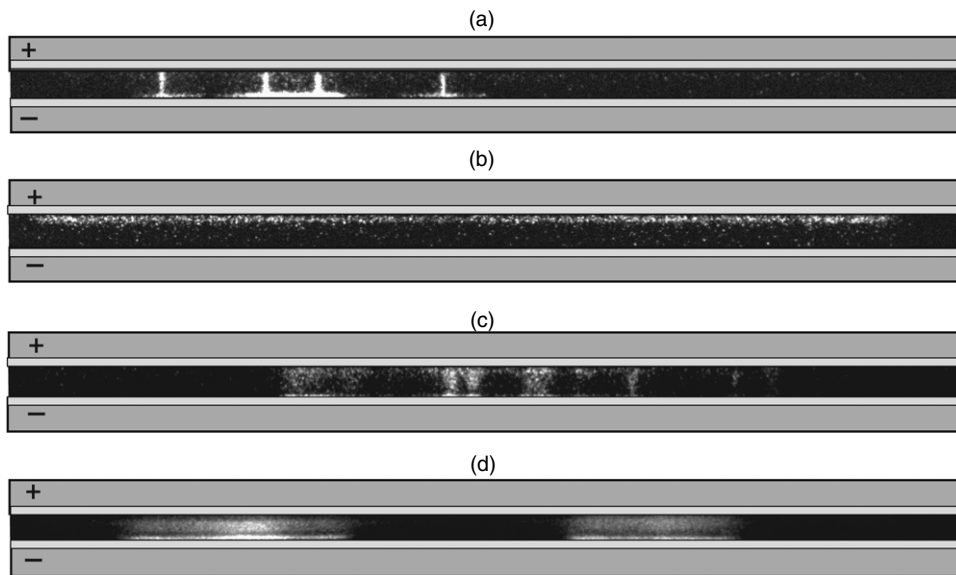


Figure 2. Different types of the DBD observed in the experiments. (a) stationary filaments; (b) Townsend discharge, (c) non-stationary microdischarges, (d) glow. The gaseous gap size is 0.9 mm and lateral size of the electrodes is 40 mm. For all the images instantaneous anode is positioned on the top and instantaneous cathode at the bottom. The exposure time is 5 ns for each image.

mainly refers to the visual appearance yet, in reality, it can correspond to different discharge types. For instance, the filamentary appearance can have an arc, glow-like discharge and positive streamer. The commonly observed filamentation of the atmospheric pressure DBD can be induced by the streamer breakdown mechanism, intrinsic instabilities of the atmospheric pressure plasma and it is also related to the parameters of external electrical circuit or the material properties of dielectric barrier, etc [22].

It is important to distinguish the terms microdischarge and filament often used in relation to DBD. In this work we are following definitions given in Fridman's textbook [23]. According to [23], the group of local processes in the discharge gap initiated by the avalanche and developing until electron current termination is called a microdischarge, while the filament in DBD is a group of microdischarges that form on the same spot each time the polarity is changed.

It is known that at high values of the electric field and large distances between the electrodes the streamer breakdown mechanism takes place instead of the uniform Townsend breakdown. The streamer breakdown occurs when the charge density in an electron avalanche becomes large enough to strongly affect the external electric field. According to the Meek criterion [24], this happens when $\alpha d > 20$, where α is the first Townsend ionization coefficient and d is the inter-electrode distance. We calculated the αd product for the voltage value of 2 kV applied to the gaseous gap of 0.6 mm (the reduced field value was overestimated compared with the experiment) in the Ar/N₂/O₂ + HMDSO gas mixture used in this study. To derive the first Townsend ionization coefficient the BOLSIG + Boltzmann equation solver [25] was applied provided with a Siglo cross-section database [26]. The ionization cross-section data for HMDSO were taken from [27]. Even with a mentioned specific field value overestimation, the calculated value of the αd product is

~ 10.4 , thus being considerably lower in comparison with 20 in the Meek criterion (given that this is an exponential factor). Therefore, streamer breakdown should not occur under the conditions of the present experiment. Nevertheless, a transition from Townsend to glow discharge modes will not necessarily takes place in a diffuse manner but can result in cathode directed (positive) streamer due to the instability of the ionization front [16]. Though the term APGD is usually attributed to the glow-like discharge with a diffuse positive column, the glow discharge at elevated pressure can also exist with the positive column contracted to a filament. The nature of such contraction is related to the Maxwellization of the electron energy distribution function [20, 28] or to a thermal instability [20].

Observation of the atmospheric pressure DBD in the above-described experimental system in the gas mixture of Ar/N₂/O₂ + HMDSO80/20/2 + 50 ppm demonstrated several types of discharges (see figure 2), namely, a discharge with stationary filaments (figure 2(a)), Townsend-like discharge APTD (figure 2(b)), non-stationary microdischarges (figure 2(c)) and a diffuse glow-like discharge APGD (figure 2(d)). The gaseous gap size for the images presented in figure 2 was 0.9 mm and the electrode area was $40 \times 12 \text{ mm}^2$. For all the images in figure 2 the instantaneous anode is positioned on the top, the instantaneous cathode at the bottom and the ICCD gate time is 5 ns. The discharges shown in figure 2 and the conditions when they appear will be discussed in the following paragraphs.

According to our observations, the discharge seen in figure 2(a), where the 'T' shaped filaments are stationary and exist for hundreds of nanoseconds, appears in the case when the dielectric barrier on one of the electrodes is damaged. The nature of damage was found to be a pinpoint defect or a burned spot resulting in conduction current at the narrow base of the 'T' shape. Those filaments can be clearly seen with the naked

eye and are reproduced at the same location in each cycle of the applied voltage.

In the described experimental cell the Townsend-like form of the discharge (figure 2(b)) was observed only as a preceding phase for a glow. No pure Townsend-like mode was seen lasting the complete duration of the discharge current pulse, probably due to the instabilities of this mode in the studied conditions (gas mixture, applied voltage and excitation frequencies). The low current APTD (figure 2(b)) appears always occupying the whole electrode area. The gradual expansion of the Townsend discharge from a certain initial point was not observed. The uniform inception of the Townsend discharge may indicate the influence of memory effects, when the residual positive ions and excited neutrals from the preceding current pulse are providing a uniform secondary electron emission over the electrode area [21].

In comparison with the filamentary discharge presented in figure 2(a), the microdischarges shown in figure 2(c) are non-stationary and the pattern formed by those microdischarges is not exactly reproducible. This means that each new image frame captured by the ICCD camera at a fixed phase of discharge voltage will show somewhat different spatial distributions of the microdischarges. The phenomena presented in figures 2(a) and (c) also need to be distinguished, because in the last case the microdischarges are not induced by any noticeable defects on the surface of the dielectric barrier. Moreover, they are not visible to the naked eye against the background of apparently uniform plasma. Note that here we are using the terms ‘filaments’ and ‘microdischarges’ according to definitions given in [23] and cited above. The dynamic evolution of the last discharge form will be described below in detail as mode 2 of discharge development. The microdischarges in figure 2(c) are characterized by the conical luminescence shape converging toward the instantaneous cathode as well as by a darker space between the cathode layer and the bulk, resembling Faraday dark space. It should be noted that converging shapes of the ionization front were also obtained in the numerical modeling for a positive streamer during the transitional stage between the Townsend and glow discharges [16].

The discharge presented in figure 2(d) can be attributed to the diffuse glow-like type, as it shows a characteristic transverse structure of the luminescence profile. In contrast to the Townsend-like mode, it occupies only a part of the electrode area, which is a recognizable property of the classical subnormal and normal glow discharges [20]. This discharge is not stationary, and its dynamic behavior will be presented below. A comparison of light emission profiles between the instantaneous cathode and the anode attributed to Townsend and glow discharges recorded for the gaseous gap of 0.9 mm in the Ar/N₂/O₂ + HMDSO gas mixture one can see in figure 3. The glow discharge is typically brighter and shows a clear structuring, which can be assigned to NG, Faraday dark space and bulk regions. As already mentioned above, the Townsend-like discharge in our experiments was observed only as a preceding phase for a glow.

We found two distinctive forms of discharge development, which are showing substantially different behavior at the

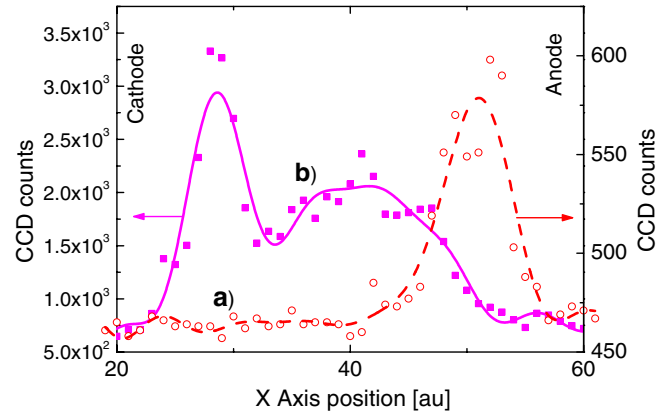


Figure 3. A transverse light emission profiles recorded from the 0.9 mm gaseous gap between the electrodes by means of fast ICCD camera at 5 ns gate time typical for (a) Townsend-like discharge and (b) glow-like discharge.

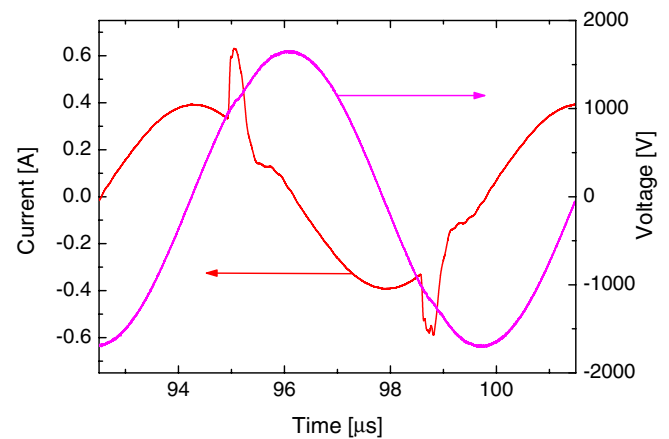


Figure 4. Current and voltage waveforms of the DBD operating in mode 1 in Ar/N₂/O₂ + HMDSO gas mixture.

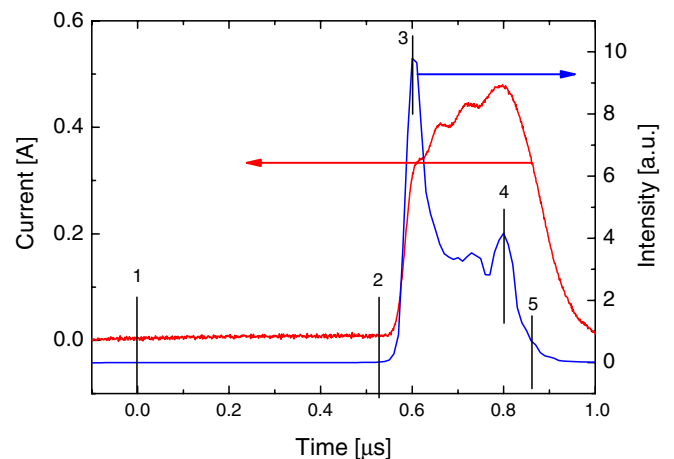


Figure 5. Current and space integrated light emission signal from the DBD in Ar/N₂/O₂ + HMDSO gas mixture operating in mode 1. The numbers on the time sections correspond to the numbered ICCD frames in figure 6.

nanosecond time scale. One of those forms (mode 1) which we are attributing to a high current density glow-like discharge is presented in figures 4–6. In figure 4 the voltage–current waveforms of the discharge are shown. In figure 5 we

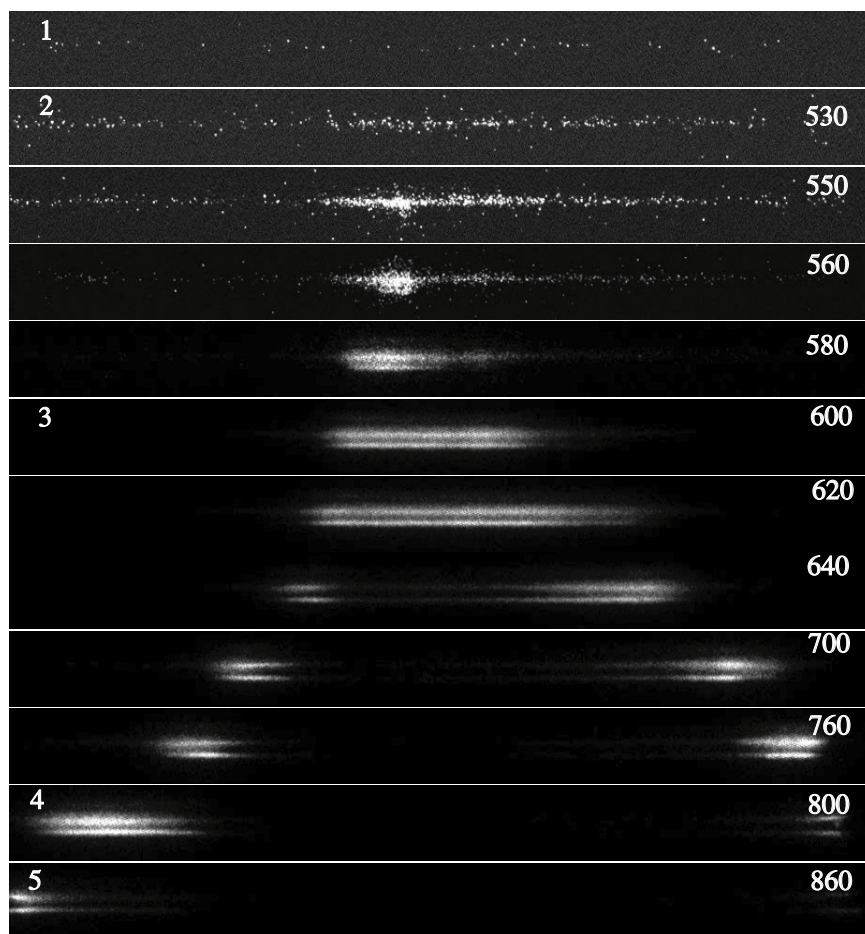


Figure 6. ICCD frame sequence of the DBD in Ar/N₂/O₂ + HMDSO gas mixture corresponding to the current waveform in figure 5. The image delay time in nanoseconds relative to the first frame is also reported at the right side. The exposure time is 10 ns for each frame. The instantaneous cathode is on the bottom and anode is on the top. The gaseous discharge gap is 0.6 mm and the lateral size of the electrodes is 40 mm.

present the discharge current corrected for the main harmonic component of the displacement current and the total intensity of broadband emission from the discharge (obtained by the integration of raw data from the ICCD sensor). The dynamic discharge evolution is shown in figure 6, where each separate image frame was recorded at the ICCD gate time of 10 ns. The measurements were carried out in the Ar/N₂/O₂/HMDSO (80 : 20 : 2 +50 ppm) gas mixtures and under power density conditions typical for the deposition of the silica-like films [3, 4]. The gaseous gap size for this experiment was 0.6 mm. ICCD photographs indicate the discharge appearance (breakdown of gaseous gap) a few hundred nanoseconds before the main current and luminescence pulse. The spatial distribution of the early luminescence signal (the light comes from the region near the anode and the light emission is distributed over the whole electrode area) points out that this initial stage can be attributed to the dark or Townsend-like discharge. It can be expected that in the case of atmospheric pressure DBD at a frequency range of ~ 100 kHz and higher and a gap distance of ~ 1 mm, the positive ions are trapped in the discharge gap as the ion drift time to the surface is of the same order as the period of the applied voltage. The space charge formed by the positive ions, which were produced during the preceding glow-like phase, would affect the electric

field profile at the ignition of the next discharge. Therefore, the uniform field across the gap (typical for a classical Townsend discharge) is hardly to be realized in the continuously running DBD under the conditions of the present experiment.

The current density of the Townsend-like discharge is low (typically not exceeding 1 mA cm^{-2} , see also [29]) and in the present experimental arrangement with a small discharge area it cannot be clearly distinguished from the noise. As the current density of the Townsend-like discharge increases, a transition to the glow mode occurs accompanied by a local jump in charged particle densities, discharge current and luminescence intensity by a few orders of magnitude. This can be seen by the steep increase in the current and fluorescence signal in figure 5.

The glow-like discharge development scenario presented in figures 5 and 6 is characterized by the significant light intensity peak, approximately 50–100 ns broad, at the start of the glow-spot formation which was not followed by the current wavelike shape. This phenomenon can be an interesting topic for further time-resolved OES investigation of the excitation kinetics in atmospheric discharge. In the high current density mode we observed the formation of one or two bright current spots which move along the lateral direction between the electrodes. The dynamic expanding behavior of the plasma can be explained by the following considerations. After initial

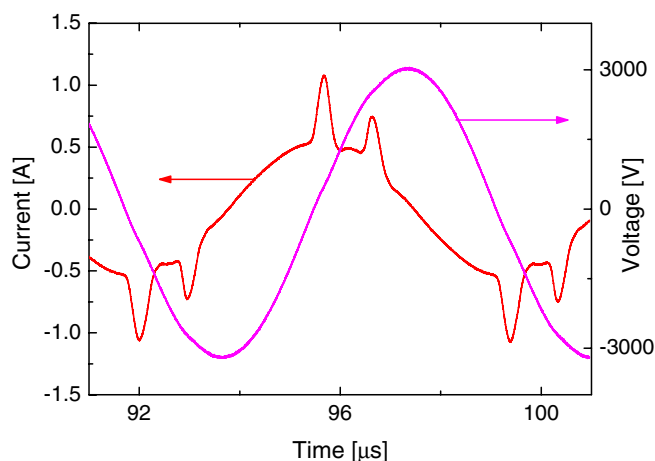


Figure 7. Current and voltage waveforms of the DBD operating in mode 2 in Ar/N₂/O₂ + HMDSO gas mixture.

formation of the glow-like spot, surface charge is quickly deposited on the dielectric, strongly reducing the local electric field. The resulting field becomes too low to support the ionization and plasma starts to recombine. However, the transverse electric field is still high at the radial periphery of the initial current spot, providing a development of the ‘retarded’ transverse ionization wave which results in the lateral expansion of the glow observed in the experiment. The radial expansion of the glow current spot was previously investigated for DBD in helium [14, 15], yet in our work we are able to follow and distinguish the transition between Townsend and glow modes of the discharge, as well as to sustain high current atmospheric glow in non-He based gas mixture in a depositing plasma.

One can see the modulation on the discharge current waveshape followed by the variations of the luminosity (figure 5). In our experiments this non-monotonic behavior was often observed in the presence of HMDSO. This can be related to the fact that in a depositing plasma gas composition is not uniform along the gas flow direction due to the precursor dissociation and consumption via thin film deposition on the dielectric. The surface properties of the dielectric, for instance the secondary emission of electrons, change as well because of the deposition process. All this can result in irregularities in the horizontal propagation of the ionization wave. The estimated value for the instantaneous current density in this regime is in the order of 0.7 A cm^{-2} , being approximately three orders higher than the characteristic values for the Townsend-like discharge. For a more accurate determination of the current density and a test whether the constant normal current density effect holds [20], a system with transparent electrodes would be necessary.

Another development scenario (mode 2) can be seen in figures 7-9. In figure 7 the voltage–current characteristics of the discharge is shown. In this case two current peaks per half-period of applied voltage are observed. A diffuse atmospheric DBD with more than one current peak per half-period is sometimes referred to as a pseudoglow discharge [10, 30]. Figure 8 demonstrates one of the discharge current peaks (again corrected for the main harmonic component of

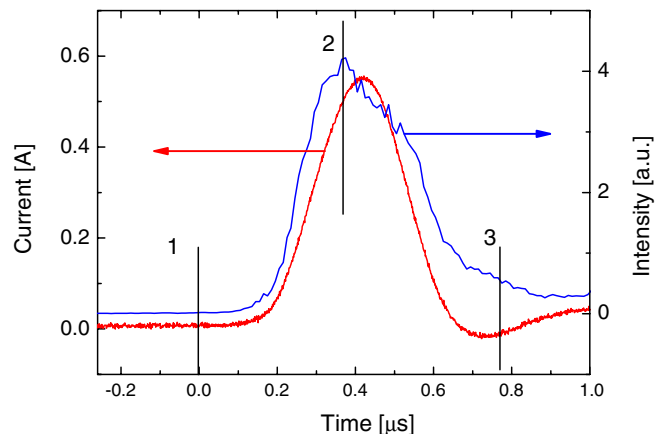


Figure 8. Current and space integrated light emission signal from the DBD in Ar/N₂/O₂ + HMDSO gas mixture operating in mode 2. The numbers on the time sections correspond to the numbered ICCD frames in figure 9.

the displacement current) and the total intensity of broadband light emission from the discharge. Figure 9 shows the ICCD frames representing discharge evolution in time corresponding to the current peak shown in figure 8. The gaseous gap size for this experiment was 1.2 mm. In this case one can see the simultaneous formation of the multiple microdischarges over a relatively large area in the gap between the electrodes. The density of the microdischarges increases with time. Eventually, starting from 220 ns delay time (see figure 9) a diffuse appearance is formed. However, the light emission pattern does not correspond to what is expected for a glow discharge. The characteristic property of this discharge mode is the presence of the relatively bright sheath near the instantaneous anode. Because the discharge in this regime is occupying a large electrode area the instantaneous current density will be lower when compared with the previously described regime even if the total discharge current is relatively high. The estimated current density value is 0.15 A cm^{-2} for point 2 indicated in figures 8 and 9. To the naked eye the visual appearance of this form can be similar to the glow-like mode shown in figure 6.

It should be mentioned that the discharge evolution pattern presented in figure 6 has a trend to be observed often but not exclusively at smaller discharge gap sizes while development demonstrated in figure 9 is more characteristic for larger separation of the electrodes. Alternatively, the glow-like discharge can be initiated by the filamentary discharge. We have already reported this unusual behavior in [19].

It is important to note that, although the present fast imaging investigation was performed for a relatively small discharge cell, the similar discharge development patterns were also observed in the case of larger electrode areas, under the conditions of the thin film deposition experiment presented in [3, 4]. However, in the last case the transverse structure of the discharge in the submillimeter gaseous gap cannot be resolved, and also the initial location of the glow-like current spot appearance is less defined.

It was proposed in [29] using the example of a DBD in nitrogen that for the formation of the diffuse atmospheric

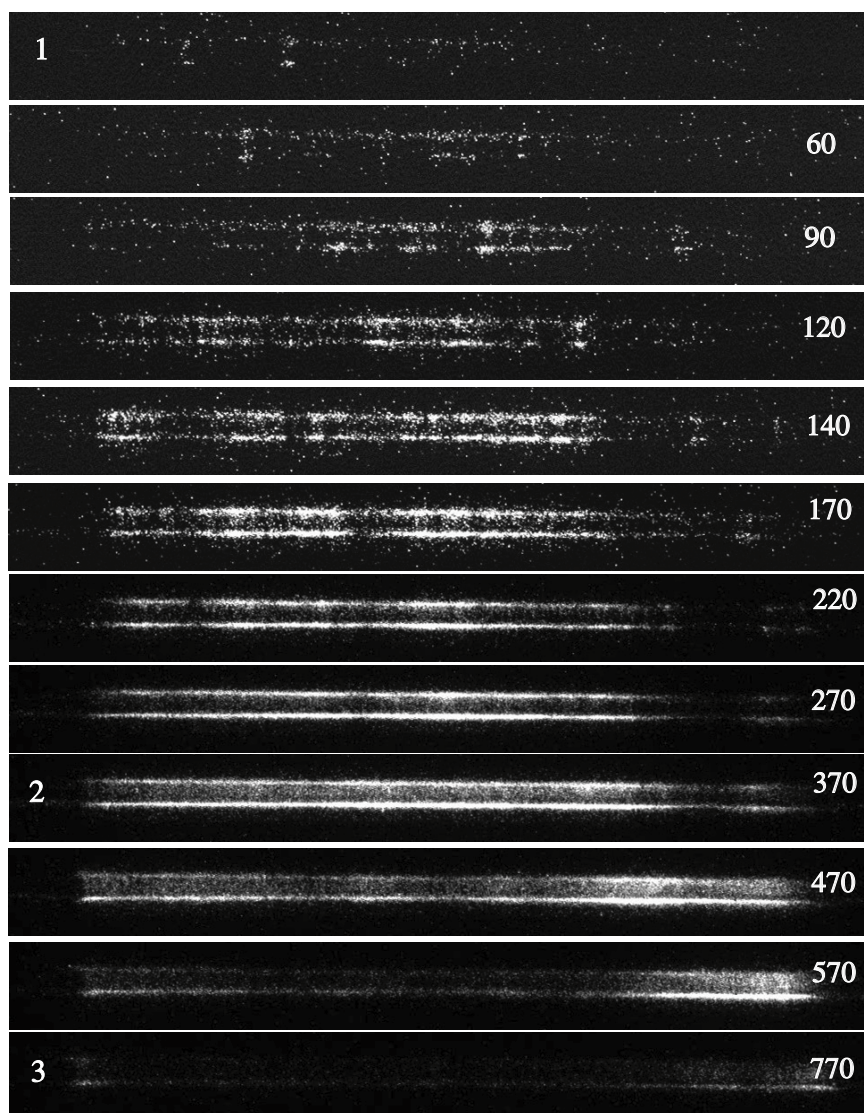


Figure 9. ICCD frame sequence of the DBD in Ar/N₂/O₂ + HMDSO gas mixture, corresponding to the current waveform in figure 8. The image delay time in nanoseconds relative to the first frame is also reported at the right side. The exposure time is 10 ns for each frame. The instantaneous cathode is on the top and anode is on the bottom. The gaseous discharge gap is 1.2 mm and the lateral size of the electrodes is 40 mm.

plasma it is necessary to have a uniform pre-ionization that can occur via the associative ionization process involving N₂A³Σ_u⁺ metastable excited states. Alternatively, it was discussed in [21] that the flux of nitrogen metastable states on the cathode may result in a substantial and uniform emission of secondary electrons, attached in shallow traps on the dielectric surface, which in this way contribute to the appearance of the diffuse discharge. The molecular excited states are accumulating during the preceding current pulses. The addition of oxygen into the gas mixture results in efficient quenching of the N₂A³Σ_u leading to a non-uniform discharge as directly observed in [31] using an optical–optical double resonance-LIF technique (OODR-LIF) for the absolute measurements of the N₂A³Σ_u density. It is important to note that this mechanism should be considered for the low current Townsend-like discharge. It was already demonstrated in [22] that the pre-ionization is not a necessary condition for diffusive glow formation. This work directly shows that

the diffuse glow-like discharge can be ignited in the mixture with a considerable oxygen content. This indicates that the diffuse glow-like DBD mode is not only characterized by the high specific power dissipation but is also more stable toward gas content and initial conditions when compared with the Townsend-like discharge.

4. Conclusions

It has been demonstrated that atmospheric pressure plasma-enhanced chemical vapor deposition system studied in this work can operate in the diffuse glow-like discharge mode in He-free gas mixtures with a considerable oxygen content. The glow-like discharge type was identified by the light emission pattern showing NG, Faraday dark space and bulk regions. This observation was complemented by the measurements of the substantial instantaneous current density of ~0.7 A cm⁻². Alternatively it was also seen that visually uniform discharge

can be initiated by the large number of the microdischarges indistinguishable by the naked eye. The formation process of the glow-like mode includes initial uniform Townsend breakdown of the gaseous gap, the Townsend–glow transition and an expansion of the glow. The glow-like current spot is momentarily occupying only a small part of the electrode surface area; however, due to its dynamics, it provides a uniform treatment of the substrate (electrode surface) within a single unipolar current pulse for the time scale less than 1 μ s. Our recent investigations [3, 4] show that the thin silica-like films web-roll deposited in such discharge systems are characterized by very smooth morphology and low carbon content.

Acknowledgment

This research was carried out under project number MC3.06279 in the framework of the Research Program of the Materials Innovation Institute M2i (www.m2i.nl).

References

- [1] Okazaki S, Kogoma M, Uehara M and Kimura Y 1993 *J. Phys. D: Appl. Phys.* **26** 889
- [2] Massines F, Gherardi N, Fornelli A and Martin S 2005 *Surf. Coat. Technol.* **200** 1855
- [3] Starostine S, Aldea E, de Vries H, Creatore M and van de Sanden M C M 2007 *Plasma Process. Polym.* **4** S440
- [4] Antony Premkumar P, Starostin S A, de Vries H, Paffen R M J, Creatore M, Eijkemans T J, Koenraad P M and van de Sanden M C M 2009 *Plasma Process. Polym.* at press doi:10.1002/ppap200900033
- [5] Foest R, Adler F, Sigener F and Schmidt M 2003 *Surf. Coat. Technol.* **163–164** 323
- [6] O'Neill L, O'Hare L-A, Leadley S R and Goodwin A J 2005 *Chem. Vapor Depos.* **11** 477
- [7] Schmidt-Szalowski K, Rżanek-Boroch Z, Sentek J, Rymuza Z, Kusznierevicz Z and Misiak M 2000 *Plasmas Polym.* **5** 175
- [8] Fanelli F, d'Agostino R and Fracassi F 2007 *Plasma Process. Polym.* **4** 797
- [9] Trunec D, Navrátil Z, Stahel P, Zajíčková L, Buršíková V and Čech J 2004 *J. Phys. D: Appl. Phys.* **37** 2112
- [10] Morent R, De Geyter N, Van Vlierberghe S, Vanderleyden E, Dubrue P, Leys C and Schacht E 2009 *Plasma. Chem. Plasma Process.* **29** 103
- [11] Kogelschatz U 2003 *Plasma Chem. Plasma Process.* **23** 1
- [12] Fridman A, Chirokov A and Gutsol A 2005 *J. Phys. D: Appl. Phys.* **38** R1
- [13] Napartovich A P 2001 *Plasmas Polym.* **6** 1
- [14] Mangolini L, Orlov K, Kortshagen U, Heberlein J and Kogelschatz U 2000 *Appl. Phys. Lett.* **80** 1722
- [15] Haiyun Luo, Zhuo Liang, Bo Lv, Xinxin Wang, Zhicheng Guan and Liming Wang 2007 *Appl. Phys. Lett.* **91** 231504
- [16] Golubovskii Yu B, Maiorov V A, Behnke J F, Tepper J and Lindmayer M 2004 *J. Phys. D: Appl. Phys.* **37** 1346
- [17] Rahel J and Sherman D M 2005 *J. Phys. D: Appl. Phys.* **38** 547
- [18] Guikema J, Miller N, Niehof J, Klein M and Walhout M 2000 *Phys. Rev. Lett.* **85** 3817
- [19] Starostin S A, ElSabbagh M A M, Aldea E, de Vries H, Creatore M and van de Sanden M C M 2008 *IEEE Trans. Plasma Sci.* **36** 968
- [20] Raizer Yu P 1991 *Gas Discharge Physics* (Berlin: Springer)
- [21] Massines F, Gherardi N, Naude N and Segur P 2008 *Proc. 11th Int. Symp. on High Pressure Low Temperature Plasma Chemistry (Hakone 11, Japan)* (France: Université Paul Sabatier) p 21
- [22] Aldea E, Peeters P, de Vries H and van de Sanden M C M 2005 *Surf. Coat. Technol.* **200** 46
- [23] Fridman A 2008 *Plasma Chemistry* (New York: Cambridge University Press)
- [24] Meek J M and Craggs J D 1978 *Electrical Breakdown of Gases* (New York: Wiley)
- [25] Hagelaar G J M and Pitchford L C 2005 *Plasma Sources Sci. Technol.* **14** 722
- [26] Boeuf J P, Pitchford L C and Morgan W L 1998 *The Siglo Database* <http://www.siglo-kinema.com>
- [27] Basner R, Foest R, Schmidt M, Becker K and Deutsch H 1998 *Int. J. Mass Spectrom.* **176** 245
- [28] Dyatko N A, Ionikh Y Z, Kochetov I V, Marinov D L, Meshchanov A V, Napartovich A P, Petrov F B and Starostin S A 2008 *J. Phys. D: Appl. Phys.* **41** 055204
- [29] Gherardi N, Gouda G, Gat E, Ricard A and Massines F 2000 *Plasma Sources Sci. Technol.* **9** 340
- [30] Radu I, Bartnikas R and Wertheimer M R 2003 *IEEE Trans. Plasma Sci.* **31** 1363
- [31] Dilecce G, Ambrico P F and De Benedictis S 2007 *Plasma Sources Sci. Technol.* **16** 511